INTERNATIONAL JOURNAL OF
NUMERICAL ANALYSIS AND MODELING
Volume 6, Number 4, Pages 627–641

AN UNCONDITIONALLY STABLE SECOND ORDER METHOD FOR THE LUO-RUDY 1 MODEL USED IN SIMULATIONS OF DEFIBRILLATION

MONICA HANSLIEN, ROBERT ARTEBRANT, JOAKIM SUNDNES AND ASLAK TVEITO

Abstract. Simulations of cardiac defibrillation are associated with considerable numerical challenges. The cell models have traditionally been discretized by first order explicit schemes, which are associated with severe stability issues. The sharp transition layers in the solution call for stable and efficient solvers. We propose a second order accurate numerical method for the Luo-Rudy phase 1 model of electrical activity in a cardiac cell, which provides sequential update of each governing ODE. An *a priori* estimate for the scheme is given, showing that the bounds of the variables typically observed during electric shocks constitute an invariant region for the system, regardless of the time step chosen. Thus the choice of time step is left as a matter of accuracy. Conclusively, we demonstrate the theoretical result by some numerical examples, illustrating second order convergence for the Luo-Rudy 1 model.

Key Words. unconditionally stable, second order method, maximum principle, defibrillation, ODE system

1. Introduction

Computer simulations of cardiac electrophysiology have been established as a helpful tool, particularly in the study of defibrillation where it is hard to observe what is going on through *in vitro* experiments. The simulations are typically based on a system of two PDEs, named the bidomain model of electrical activity in the heart. Normally these equations are coupled to a set of ODEs, which serve to describe the electrochemistry of a single cardiac cell. There is an ever increasing need for efficient numerical methods as the mathematical models tend to expand in size and complexity along with a higher level of realism. However, older cell models such as the Beeler-Reuter model [1] and the Luo-Rudy phase 1 (LR1) model [8] are also commonly used in simulations that involve electric shocks, and serve to describe the electrophysiological membrane dynamics in a fairly realistic way.

Traditional numerical methods used in simulations of cardiac defibrillation are based on forward Euler integrators with poor stability properties. These stability issues are a consequence of the high values that the transmembrane potential undertakes when the electric shock is on, as addressed in [4]. In that study, a numerical method for the LR1 model of order $O(\Delta t)$ was presented. This scheme was proved to be unconditionally stable, leaving the choice of time step as a matter of accuracy. However, the extremely sharp transition layers in the solution present during strong electric shocks put particularly high demands on the accuracy and stability of the solvers. Also, in the strive for realistic simulations of defibrillation one would

Received by the editors September 4, 2008, in revised form, February 3, 2009.
This work was partly supported by the Research Council of Norway.

need to solve the equations on 3D geometries with relatively high resolution. Due to these challenges, a numerical method that admits second order accuracy would save considerable computation time. When we are to solve the coupled system of ODEs and PDEs, it is possible to use an operator splitting technique in time which is of order $O(\Delta t^2)$, see [10] and [13]. Therefore, it would be desirable for the ODE solver to preserve the level of accuracy. In the present paper, we propose a second order accurate method for the LR1 model. The numerical scheme is based on a quasi-implicit method, which makes it possible to solve each ODE in separate, where a method of Rush-Larsen type [11] is used for integration of the resulting linear equation, together with a Lobatto IIIC method for the governing equation of the scaled calcium concentration. A maximum principle for this scheme reveals that the numerical solutions yield no numerical instabilities, regardless of the time-step chosen. Thus we have a stable numerical method for the ODE system with the same level of accuracy as can be obtained at the PDE level.

The rest of the paper is organised as follows. In Section 2 we present the mathematical model under consideration, and in Section 3 we derive the numerical method. *A priori* bounds of this scheme are given in Section 4, before we show some simulation results in Section 5.

2. Model equations

Propagation of an electrical pulse in the heart can be formulated mathematically by the bidomain model, and is thoroughly described in [5, 14]. The cardiac tissue is divided into extracellular (e) and intracellular (i) domains, on which the electrical potential is represented by u_e and u_i, respectively. We may then write the transmembrane potential in terms of these two quantities as $v = u_i - u_e$, measured in mV. Moreover, M_i and M_e are conductivity tensors for the intra- and extracellular space, and s is a model dependent state vector. The complete system reads

$$\frac{\partial s}{\partial t} = P(s, v), \tag{1}$$

$$\frac{\partial v}{\partial t} + I_{ion}(v, s) = \nabla \cdot (M_i \nabla v) + \nabla \cdot (M_i \nabla u_e), \qquad x \in H, \tag{2}$$

$$0 = \nabla \cdot (M_i \nabla v) + \nabla \cdot ((M_i + M_e) \nabla u_e), \qquad x \in H, \tag{3}$$

where we have denoted by H our computational domain.

In the simulations we use the boundary conditions presented in [3] wherever the heart is under normal electrophysiological conditions, whereas we incorporate the electric shock as Dirichlet conditions during some time interval $t \in [t_1, t_2]$. The shock is placed on the heart surface, but one could easily extend the model to include torso simulations with the shock delivered through external electrode pads on the surface of the body. For an outer normal vector n_H we set

$$n_H \cdot M_i \nabla (u_e + v) = 0, \ x \in \partial H_1, \tag{4}$$

$$n_H \cdot M_i \nabla (u_e + v) = 0, \ x \in \partial H_2 \cup \partial H_3, \ t < t_1 \text{ or } t > t_2, \tag{5}$$

$$u_e = u_1, \ x \in \partial H_2, \ t_1 \le t \le t_2, \tag{6}$$

$$u_e = u_2, \ x \in \partial H_3, \ t_1 \le t \le t_2, \tag{7}$$

where the values of the shock are given by u_1 (cathode) and u_2 (anode).

Equation (1) is a system of ODEs which describes electrical kinetics of a single cell, and in the present study we let this represent the Luo-Rudy phase 1 model [8]. This cell model comprises eight variables, including the transmembrane potential v,

the scaled intracellular calcium concentration $c = 10^3[Ca^{2+}]_i$, as well as six gating variables denoted by $y = m, h, j, f, d, X$. Both depolarization and the refractory phase can be fairly well described by this system, which reads

$$\frac{dv}{dt} = -I_{ion}(v, c, m, h, j, f, d, X), \tag{8}$$

$$\frac{dc}{dt} = 0.07(10^{-4} - c) - 10^{-4} I_{si}(v, c, f, d), \tag{9}$$

$$\frac{dy}{dt} = \alpha_y(v)(1 - y) - \beta_y(v)y, \quad y = m, h, j, f, d, X. \tag{10}$$

The gate variables control the flow of ions across the membrane, and α_y, β_y, $y = m, h, j, f, d, X$, are positive functions that represent the opening and closing rates of the gates, see Appendix A for the expressions.

Inactivation of the sodium current, I_{Na}, contains two gate variables, h and j, which have rate constants that are formulated as discontinuous functions of v. Generally, when we are to solve an ODE of the type

$$\frac{dy}{dt} = G(y)$$

with a second order method, the order of accuracy will be destroyed if there are discontinuities in G. For the Luo-Rudy 1 model, there are jumps in the rate functions for $v = -40$mV. Therefore we have replaced these with smooth approximations, found by a MATLAB curvefit toolbox using data from the original rate functions. All the rate functions used in the simulations are listed in Appendix A.

The total ionic current across the cell membrane, I_{ion}, is given by

$$\begin{aligned} I_{ion}(v, c, m, h, j, f, d, X) = {} & I_{Na}(v, m, h, j) + I_{K1}(v) + I_K(v, X) \\ & + I_{Kp}(v) + I_b(v) + I_{si}(v, f, d, c). \end{aligned} \tag{11}$$

Below we have listed the expressions for the individual currents that appear in (11). For convenience, we gather the constant conductivities together with the gate variables of each component so that the gating mechanisms are collected into Y_w, $w = si, Na, K, K1, Kp, b$, as follows

$$\begin{aligned} I_{si}(v, f, d, c) &= Y_{si}(v - E(c)), \quad Y_{si} = g_s f d, \\ \text{with} \quad E(c) &= 7.7 - 13.0287 \ln(c), \\ I_K(v, X) &= Y_K(v - E_K), \quad Y_K = g_K X X_i, \\ I_{K1}(v) &= Y_{K1}(v - E_{K1}), \quad Y_{K1} = g_{K1} K1_\infty, \\ I_{Kp}(v) &= Y_{Kp}(v - E_{Kp}), \quad Y_{Kp} = g_{Kp} Kp, \\ I_b(v) &= Y_b(v - E_b), \quad Y_b = g_b, \\ I_{Na}(v, m, h, j) &= Y_{Na}(v - E_{Na}), \quad Y_{Na} = g_{Na} m^3 h j. \end{aligned}$$

The equilibrium potentials E_w and the membrane conductivities g_w, for $w = Na, K, K1, Kp, b$, as well as g_s, are all constants whose values are given in Table 5. We remark that in simulations of cardiac defibrillation, it is common to extend the ODE system with an additional equation for electroporation of the cell membrane, as was done in [4]. Since the analysis in that study can be directly transferred to the present work, we have left out the electroporation function. We also remark that several models for electroporation of cells exist, see e.g. [6, 7, 2].

3. Numerical method

Equations (1)-(7) constitute a complicated system which is hard to solve fully coupled. To reduce the level of complexity, an operator splitting technique in time is commonly used to obtain a set of ODEs and a system of PDEs which are to be solved separately. A solution of second order accuracy in time can be obtained for the PDE system by the Strang splitting technique described in [10], and for the bidomain model this can be done as discussed in [13]. It would be preferable to have an ODE solver that preserves this level of accuracy, so we present a second order method for the ODE system (8)-(10). A tempting choice is the Crank-Nicolson scheme which is of second order accuracy. However, if we perform a stability analysis in terms of showing bounds on the discrete solutions, we find that the time step restriction becomes only twice as large as that of the forward Euler method investigated in [4]. Then Δt still needs to be in the order of 10^{-27}ms, due to the strong shocks, which makes this scheme unfit for the LR1 model used in such simulations. Other second order schemes like the BDF scheme or the second order SDIRK method are relatively easy to implement, but they are hard to analyze in terms of proving a priory bounds for solutions in the range of defibrillation. Below we present a second order ODE solver which is unconditionally stable, even during defibrillation.

The discretization of equations (8)-(10) is based on a quasi-implicit scheme, i.e. in each governing ODE for the membrane potential as well as for the gates, the variable subject to change is evaluated explicitly whereas the scaled calcium concentration admits implicit evaluation at each time increment. The other variables on the right hand sides in all the equations are just inputs from the previous time step. Consequently, for each time evaluation, all equations in the ODE system become decoupled and can be solved separately. The resulting one-variable ODEs for the transmembrane potential as well as for the gating variables then become linear, so that the integration method of Rush and Larsen [11] can be applied. A two stage Lobatto IIIC type implicit Runge-Kutta method is applied to the ODE for the scaled calcium concentration.

For the gating variables we find

$$\frac{dy}{dt} = (1-y)\alpha_y(v^n) - \beta_y(v^n)y, \quad y = m, h, j, f, d, X,$$

which is linear in y. The governing equation for the transmembrane potential is not linear in v since the terms Y_{K1}, Y_K and Y_{Kp} on the right hand side are functions of the conductance parameters $K1_\infty(v)$, $X_i(v)$ and $K_p(v)$ respectively, which are explicit functions of v. The equation for the transmembrane potential can however be linearized by simply evaluating the conductance parameters from the previous time step; all the other variables are taken from the previous evaluations as well. In this way we obtain a linear ODE in v

$$\begin{aligned}\frac{dv}{dt} =& Y^n_{Na}(E_{Na} - v) + Y^n_{K1}(E_{K1} - v) + Y^n_K(E_K - v) + \\ & Y^n_{Kp}(E_{Kp} - v) + Y^n_b(E_b - v) + Y^n_{Si}(E(c^n) - v)\,, \end{aligned} \tag{12}$$

which is easily integrated exactly. Consequently, the equations for the gates and the transmembrane potential can be written on the form

$$\frac{du}{dt} = a^n - b^n u, \tag{13}$$

where a and b are constants in each time step n. Due to the form of (13), the equations can be solved analytically for each time step. We use an integration of Rush-Larsen type which gives update like

$$u^{n+1} = \frac{a^n}{b^n} + (u^n - \frac{a^n}{b^n})e^{-b^n \Delta t}. \tag{14}$$

Note that this is the exact solution of (13) after one time increment. For simplicity we shall define

$$Y_E^n = Y_{Na}^n E_{Na} + Y_{K1}^n E_{K1} + Y_K^n E_K + Y_{Kp}^n E_{Kp} + Y_b E_b + Y_{si}^n E(c^n) \tag{15}$$

and

$$Y_I^n = Y_{Na}^n + Y_{K1}^n + Y_K^n + Y_{Kp}^n + Y_b + Y_{si}^n, \tag{16}$$

such that (12) takes the form

$$\frac{dv}{dt} = Y_E^n - Y_I^n v.$$

In order to obtain the desired level of accuracy, we need to evaluate all solutions twice between t_n and t_{n+1}. First we use (14) with step size $\frac{\Delta t}{2}$ in order to find an intermediate solution set at time $t_{n+\frac{1}{2}}$. In the next round we feed the solutions found at $t_{n+\frac{1}{2}}$ into the right hand side of (14), again except from the variable subject to change. Then, with a time increment of Δt, we integrate to obtain a solution set at time t_{n+1}. A Taylor series analysis shows that in order to obtain a formally second order accurate approximation, the intermediate solution needs only to be approximated to first order. This is exploited in the scheme for the calcium concentration, see below. The procedure can be summarised as follows:

Step 1 Compute $v^{n+\frac{1}{2}}, y^{n+\frac{1}{2}}, c^{n+\frac{1}{2}},\ y = m, h, j, f, d, X$. With v evaluated at time t_n, calculate

$$y^{n+\frac{1}{2}} = y_\infty^n + (y^n - y_\infty^n)e^{-(\alpha(v^n)+\beta(v^n))\frac{\Delta t}{2}} \tag{17}$$

where

$$y_\infty^n = \frac{\alpha(v^n)}{\alpha(v^n) + \beta(v^n)}.$$

Moreover, using $c^n, y^n,\ y = m, h, j, f, d, X$ compute

$$v^{n+\frac{1}{2}} = \frac{Y_E^n}{Y_I^n} + (v^n - \frac{Y_E^n}{Y_I^n})e^{-Y_I^n(\frac{\Delta t}{2})}. \tag{18}$$

The calcium concentration in the first half step can be found by a standard backward Euler method, since only first order accuracy is needed. Find $c^{n+\frac{1}{2}}$, with v^n, f^n, d^n as input on the right hand side, i.e. calculate

$$\frac{c^{n+\frac{1}{2}} - c^n}{\Delta t/2} = F(v^n, f^n, d^n, c^{n+\frac{1}{2}}) \tag{19}$$

where

$$F(v, f, d, c) = 0.07(10^{-4} - c) - 10^{-4}\big(Y_{si}(v - E(c))\big). \tag{20}$$

This gives a nonlinear equation for $c^{n+\frac{1}{2}}$ which is solved with a Newton method. Next use the solutions evaluated in the half step as input to the calculations of the full time step;

Step 2 Compute $v^{n+1}, c^{n+1}, y^{n+1},\ y = m, h, j, f, d, X$. Calculate

$$y^{n+1} = y_\infty^{n+\frac{1}{2}} + (y^n - y_\infty^{n+\frac{1}{2}})e^{-(\alpha(v^{n+\frac{1}{2}})+\beta(v^{n+\frac{1}{2}}))\Delta t} \tag{21}$$

where v is evaluated at $t_{n+\frac{1}{2}}$, and

$$v^{n+1} = \frac{Y_E^{n+\frac{1}{2}}}{Y_I^{n+\frac{1}{2}}} + (v^n - \frac{Y_E^{n+\frac{1}{2}}}{Y_I^{n+\frac{1}{2}}})e^{-Y_I^{n+\frac{1}{2}}\Delta t}, \tag{22}$$

where all $c, y,\ y = m, h, j, f, d, X$ are evaluated at time $t_{n+\frac{1}{2}}$.

Also, in (22), we have found $Y_E^{n+\frac{1}{2}}, Y_I^{n+\frac{1}{2}}$ by first calculating $K1_\infty(v^{n+\frac{1}{2}}), X_i(v^{n+\frac{1}{2}})$ and $K_p(v^{n+\frac{1}{2}})$. Finally, solve the nonlinear ODE

$$\frac{dc}{dt} = F(v^{n+\frac{1}{2}}, f^{n+\frac{1}{2}}, d^{n+\frac{1}{2}}, c), \tag{23}$$

where F is defined by (20). It remains to find a suitable second order scheme for (23). As mentioned above, the Crank-Nicolson method provides poor stability properties so instead we have chosen a Lobatto IIIC scheme. This approach involves solving a coupled system of two intermediate stages and gives, formally, second order accuracy in time. The Lobatto IIIC method has the Butcher tableau

$$\begin{array}{c|cc} 0 & \frac{1}{2} & -\frac{1}{2} \\ 1 & \frac{1}{2} & \frac{1}{2} \\ \hline & \frac{1}{2} & \frac{1}{2} \end{array},$$

and for the ODE the scheme reads

$$\begin{aligned} k_1 &= F\left(c_n + \frac{1}{2}\Delta t k_1 - \frac{1}{2}\Delta t k_2\right) \\ k_2 &= F\left(c_n + \frac{1}{2}\Delta t k_1 + \frac{1}{2}\Delta t k_2\right) \\ c_{n+1} &= c_n + \frac{1}{2}\Delta t k_1 + \frac{1}{2}\Delta t k_2\,. \end{aligned}$$

Observe that the sequential nature of the numerical method for the entire ODE system, makes the equations easy to analyse separately, in terms of finding bounds on solutions.

4. A maximum principle

In the following we prove that the solutions generated by the scheme, defined by Steps 1 and 2 above, provide physiologically acceptable values, regardless of the time step chosen. Due to the operator splitting technique[13], the high potentials present during electric shocks come in as initial conditions from the PDE step and into the ODE system. Therefore it is crucial to check that the ODE solver handles these values. In [4] we motivated the bounds of the transmembrane potential as well as the calcium concentration. The same argument for both variables applies here as well. We found the maximum and minimum values (in mV) for the membrane potential to be

$$v^+ = 800 \quad \text{and} \quad v^- = -800, \tag{24}$$

which are close to the values observed in experimental studies of defibrillation, see [7] and references therein. For the scaled calcium concentration we set the lower and upper bounds

$$c^- = e^{\frac{7.7-v^+}{13.0287}} \approx 3.9 \cdot 10^{-27} \quad \text{and} \quad c^+ = 0.2, \tag{25}$$

respectively, where the equilibrium potential of calcium satisfies

$$E(c^-) = v^+. \tag{26}$$

Moreover, we want all the gate variables to stay within the unit interval. Thus, we state that the whole solution set should be bounded by

$$\begin{aligned} v^- \leq v^0 \leq v^+, \\ c^- \leq c^0 \leq c^+, \\ 0 \leq y^0 \leq 1, \quad y = m, h, j, f, d, X. \end{aligned} \tag{27}$$

We are now ready to prove that the numerical solution stays within the desired bounds for all time.

Theorem 4.1 (Maximum principle)**.** *Let v^n, c^n, y^n, $y = m, h, j, f, d, X$ be the solution produced by the scheme* (17) - (23)*, and let the initial conditions satisfy the bounds* (27)*. Then, for any $\Delta t > 0$*

$$v^- \leq v^n \leq v^+, \tag{28}$$

$$c^- \leq c^n \leq c^+, \tag{29}$$

$$0 \leq y^n \leq 1, \quad y = m, h, j, f, d, X, \tag{30}$$

for all $n = 0, \ldots, N$.

Proof. Assume that (28)-(30) hold for some time t_n. We start by investigating the update scheme for the gates, which reads

$$y^{n+\frac{1}{2}} = \frac{\alpha_y^n}{\alpha_y^n + \beta_y^n} + \big(y^n - \frac{\alpha_y^n}{\alpha_y^n + \beta_y^n}\big) e^{-(\alpha_y^n + \beta_y^n)\frac{\Delta t}{2}}.$$

Inserting for the upper bound of y^n gives

$$\begin{aligned} y^{n+\frac{1}{2}} &\leq \frac{\alpha_y^n}{\alpha_y^n + \beta_y^n} + \big(\frac{\alpha_y^n + \beta_y^n}{\alpha_y^n + \beta_y^n} - \frac{\alpha_y^n}{\alpha_y^n + \beta_y^n}\big) e^{-(\alpha_y^n + \beta_y^n)\frac{\Delta t}{2}} \\ &\leq \frac{\alpha_y^n}{\alpha_y^n + \beta_y^n} + \big(\frac{\alpha_y^n + \beta_y^n}{\alpha_y^n + \beta_y^n} - \frac{\alpha_y^n}{\alpha_y^n + \beta_y^n}\big) = 1, \end{aligned}$$

since

$$e^{-(\alpha_y^n + \beta_y^n)\frac{\Delta t}{2}} < 1. \tag{31}$$

Similarly, by inserting for the lower bound of y^n we find

$$\begin{aligned} y^{n+\frac{1}{2}} &= \frac{\alpha_y^n}{\alpha_y^n + \beta_y^n} + \big(y^n - \frac{\alpha_y^n}{\alpha_y^n + \beta_y^n}\big) e^{-(\alpha_y^n + \beta_y^n)\frac{\Delta t}{2}} \\ &\geq \frac{\alpha_y^n}{\alpha_y^n + \beta_y^n} - \frac{\alpha_y^n}{\alpha_y^n + \beta_y^n} e^{-(\alpha_y^n + \beta_y^n)\frac{\Delta t}{2}} \geq 0, \end{aligned}$$

where the last transition is again due to (31).

Next, consider the scheme for the transmembrane potential. Recall that

$$v^{n+\frac{1}{2}} = \frac{Y_E^n}{Y_I^n} + (v^n - \frac{Y_E^n}{Y_I^n}) e^{-Y_I^n(\frac{\Delta t}{2})}.$$

To prove the upper bound, we first observe that all $E_w,\ w = K, K1, Kp, b, Na$ are all less than the maximum of the equilibrium potential of calcium so we get

$$\begin{aligned} Y_E^n &= Y_{Na}^n E_{Na} + Y_{K1}^n E_{K1} + Y_K^n E_K + Y_{Kp}^n E_{Kp} + Y_b E_b + Y_{si}^n E(c^n) \\ &\leq (Y_{Na}^n + Y_{K1}^n + Y_K^n + Y_{Kp}^n + Y_b + Y_{si}^n) E(c^-) = Y_I^n E(c^-) = Y_I^n v^+. \end{aligned}$$

Replace v^n by its maximum value to obtain

$$v^{n+\frac{1}{2}} \leq \frac{Y_E^n}{Y_I^n} + \left(\frac{Y_I^n v^+}{Y_I^n} - \frac{Y_E^n}{Y_I^n} \right) e^{-Y_I^n (\frac{\Delta t}{2})},$$

where we realize that the terms within the parenthesis are always non-negative. Now, since

$$e^{-Y_I^n \frac{\Delta t}{2}} \leq 1, \tag{32}$$

we deduce

$$v^{n+\frac{1}{2}} \leq \frac{Y_E}{Y_I} + \left(v^+ - \frac{Y_E}{Y_I} \right) = v^+.$$

A lower bound is found in a similar manner. Realize that all equilibrium potentials are greater than the lower bound of v, so

$$Y_E^n \geq (Y_{Na}^n + Y_{K1}^n + Y_K^n + Y_{Kp}^n + Y_b + Y_{si}^n) v^- = Y_I^n v^-.$$

Consequently,

$$v^{n+\frac{1}{2}} \leq \frac{Y_E}{Y_I} + \left(v^- - \frac{Y_E}{Y_I} \right) e^{-Y_I^n \frac{\Delta t}{2}} \leq \frac{Y_E}{Y_I} + \left(v^- - \frac{Y_E}{Y_I} \right) = v^-,$$

where again we have used (32) in the last transition. As for bounds on $c^{n+\frac{1}{2}}$, we refer to [4] for details, since the analysis of this evaluation can be carried out in the exact same manner as found therein. Provided that (28)-(30) hold, we have thus shown that the solutions at time $t_{n+\frac{1}{2}}$ stay within these bounds regardless of the time step chosen. When taking a full time increment to evaluate v^{n+1}, y^{n+1}, $y = m, h, j, f, d, X$ we observe from Step 2 above that the schemes are very similar, only with input from $t_{n+\frac{1}{2}}$ instead of feeding solutions at t_n into the right hand side, and with a full time step taken. Since these values are all within the desired range, the analysis just carried out applies in the very same manner.

It remains to show bounds on c^{n+1}. Recall that the update scheme for this variable was written in Step 2 as

$$\begin{aligned} k_1 &= F\left(c^n + \frac{1}{2}\Delta t k_1 - \frac{1}{2}\Delta t k_2 \right) \\ k_2 &= F\left(c^n + \frac{1}{2}\Delta t k_1 + \frac{1}{2}\Delta t k_2 \right) \\ c^{n+1} &= c^n + \frac{1}{2}\Delta t k_1 + \frac{1}{2}\Delta t k_2 \,. \end{aligned}$$

We define

$$\begin{aligned} c_1 &= c^n + \frac{1}{2}\Delta t k_1 - \frac{1}{2}\Delta t k_2 \\ c_2 &= c^n + \frac{1}{2}\Delta t k_1 + \frac{1}{2}\Delta t k_2 \end{aligned}$$

so that $k_1 = F(c_1)$, $k_2 = F(c_2)$ and

$$c_1 = c^n + \frac{1}{2}\Delta t F(c_1) - \frac{1}{2}\Delta t F(c_2) \tag{33}$$

$$c_2 = c^n + \frac{1}{2}\Delta t F(c_1) + \frac{1}{2}\Delta t F(c_2) \tag{34}$$

with $c^{n+\frac{1}{2}} = c_2$. Reformulate the system by subtracting (33) from (34) to get the first new equation and add (33) and (34) to get the second, i.e.

$$c_2 = c_1 + \Delta t F(c_2) \tag{35}$$

$$c_2 = 2c^n - c_1 + \Delta t F(c_1)\,. \tag{36}$$

We start by observing that the right hand side of F in (20) satisfies

$$F'(c) = -0.07 - \frac{13.0287 \cdot 10^{-4} Y_{si}^{n+\frac{1}{2}}}{c} < 0\,, \quad \text{for all } c > 0 \tag{37}$$

so F is a strictly monotone function. Moreover we calculate

$$\begin{aligned} F(c^-) &= 0.07(10^{-4} - c^-) - 10^{-4} Y_{si}^{n+\frac{1}{2}}(v^{n+\frac{1}{2}} - E(c^-)) \\ &= 0.07(10^{-4} - c^-) - 10^{-4} Y_{si}^{n+\frac{1}{2}}(v^{n+\frac{1}{2}} - v^+) \geq 0.07(10^{-4} - c^-) > 0 \end{aligned}$$

and

$$\begin{aligned} F(c^+) &= 0.07(10^{-4} - c^+) - 10^{-4} Y_{si}^{n+\frac{1}{2}}(v^{n+\frac{1}{2}} - E(c^+)) \\ &\leq 0.07(10^{-4} - c^+) - 0.09 \cdot 10^{-4}(v^- - E(c^+)) \approx -6.5 \cdot 10^{-3} < 0. \end{aligned} \tag{38}$$

We shall use these facts to prove that also the calcium concentrations stay within the desired bounds for all time, regardless of the time step chosen. In order to do so we need to show that, for $c^n \in [c^-, c^+]$, the graphs of c_2 versus c_1, originating from the above equations, intersect at a point (c_1^*, c_2^*) with $c_1^*, c_2^* \in [c^-, c^+]$. Then we will have $c^{n+1} = c_2^*$ in the correct interval. Taking the derivative of (35) with respect to c_1 we find

$$\frac{dc_2}{dc_1} = \frac{1}{1 - \Delta t F'(c_2)} > 0\,,$$

for $c_2 > 0$. Similarly, for (36)

$$\frac{dc_2}{dc_1} = -1 + \Delta t F'(c_1) < 0\,,$$

for $c_1 > 0$.

We begin by showing that (35) has a solution $c_2 = c^* \in [c^-, c^+]$ for all $c_1 \in [c^-, c^+]$. Let

$$A(c_2) = c_1 - c_2 + \Delta t F(c_2)$$

such that $A(c^*) = 0$ solves (35). The derivative of A fulfills

$$A'(c_2) = -1 + \Delta t F'(c_2) < 0\,, \quad \text{for all } c_2 > 0\,.$$

Assume now that $c_1 = c^-$. Then

$$\begin{aligned} A(c^-) &= \Delta t F(c^-) > 0 \\ A(c^+) &= c^- - c^+ + \Delta t F(c^+) < \Delta t F(c^+) < 0\,, \end{aligned}$$

so we have a solution $c^* \in [c^-, c^+]$ for $c_1 = c^-$. Now, let instead $c_1 = c^+$ and find

$$A(c^-) = c^+ - c^- + \Delta t F(c^-) > \Delta t F(c^-) > 0$$
$$A(c^+) = \Delta t F(c^+) < 0\,,$$

so we have another solution $c^* \in [c^-, c^+]$ for $c_1 = c^+$. Since the derivative of (35) with respect to c_1 is positive, we will always have a solution $c^* \in [c^-, c^+]$ for all $c_1 = [c^-, c^+]$.

Next, we write equation (36) as

$$\bar{c} = 2c_n - c_1 + \Delta t F(c_1)$$

and view $\bar{c}$ as a function of c_1, $\bar{c} = \bar{c}(c_1)$. Similarly the solution to (35) is $c^* = c^*(c_1)$. Since $\dfrac{d\bar{c}}{dc_1} < 0$ for all $c_1 > 0$ and $c^* \in [c^-, c^+]$ with $\dfrac{dc^*}{dc_1} > 0$ for all $c_1 \in [c^-, c^+]$, we want to show that

(i) $\bar{c}(c^-) \geq c^*(c^-)$
(ii) $\bar{c}(c^+) \leq c^*(c^+)$

because then the two graphs intersect at the point (c_1^*, c^{n+1}), with $c_1^*, c^{n+1} \in [c^-, c^+]$. That (i) holds follows from

$$\begin{aligned}\bar{c}(c^-) - c^*(c^-) &= 2c_n - c^- + \Delta t f(c^-) - (c^- + \Delta t F(c^*)) \\ &= 2(c_n - c^-) + \Delta t(F(c^-) - F(c^*)) \geq \Delta t(F(c^-) - F(c^*)) \geq 0\end{aligned}$$

since $c^*, c^n \in [c^-, c^+]$ and $F'(x) < 0$ for all positive x. Similarly, we find that the second statement holds since

$$\begin{aligned}c^*(c^+) - \bar{c}(c^+) &= c^+ + \Delta t F(c^*) - (2c_n - c^+ + \Delta t F(c^+)) \\ &= 2(c^+ - c_n) + \Delta t(F(c^*) - F(c^+)) \geq \Delta t(F(c^*) - F(c^+)) \geq 0\,.\end{aligned}$$

Thus we have a unique solution $c^{n+1} \in [c^-, c^+]$, where the bounds are as defined in (25). In view of the above lines of argument, we state that the entire solution set at time t_{n+1} satisfies

$$\begin{aligned}v^- \leq v^{n+1} \leq v^+, \\ c^- \leq c^{n+1} \leq c^+, \\ 0 \leq y^{n+1} \leq 1, \quad y = m, h, j, f, d, X.\end{aligned}$$

Now, since the solutions are within these bounds initially, the proof is concluded by induction on n. □

5. Numerical experiments

In order to illustrate that our proposed method is second order accurate and that it actually provides unconditional stability, we will in this section present some numerical experiments. The system of ODEs, (8)-(10), that constitutes the original LR1 model is solved with the two steps outlined in Section 3. Since it is impossible to obtain an analytical solution of the ODE model, we find a reference solution by computing an extremely fine solution set denoted by $u = (v, c, y),\ y = m, h, j, f, d, X$. To calculate this we use a built-in MATLAB solver, `ode15s`. The solution obtained with the second order method is denoted by $u_\Delta = (v, c, y)_\Delta,\ y = m, h, j, f, d, X$. Then we measure the l_2-norm of the difference between u and u_Δ

at time $t = 10$ms. We define the l_2-norm to be

$$\|u - u_\Delta\|_2 = \big((v - v_\Delta)^2 + (c - c_\Delta)^2 + \sum_y (y - y_\Delta)^2\big)^{\frac{1}{2}}, \tag{39}$$

for $y = m, h, j, f, d, X$. Tables 1 and 2 show convergence results for the method

Δt	1.order scheme			2.order scheme		
(ms)	error	rate	constant	error	rate	constant
2^{-3}	1.097e-01	2.8251	0.88	2.27e-01	2.78	74.1
2^{-4}	5.80e-02	0.92	0.93	7.33e-02	1.63	6.71
2^{-5}	8.20e-02	-0.50	2.63	1.85e-02	1.99	18.1
2^{-6}	5.72e-02	0.52	3.67	4.67e-03	1.99	18.0
2^{-7}	2.93e-02	0.97	3.74	1.18e-03	1.99	18.0
2^{-8}	1.74e-02	0.75	4.46	2.96e-04	1.99	18.5
2^{-9}	9.20e-03	0.95	4.58	7.43e-05	2.00	18.9
2^{-10}	4.80e-03	0.94	4.92	1.86e-05	2.00	19.2

TABLE 1. Errors at $t = 10$ (ms) for the initial data $(v = -40, c = 0.0002, m = 0, h = 1, j = 1, X = 0, d = 0, f = 1)$.

under consideration. For comparison, we have included convergence results for our first order accurate method described in [4]; Table 1 displays the error for several values of Δt. The solution is initially set to $(v, c, m, h, j, f, d, X)_{t=0} = (-40, 2 \cdot 10^{-4}, 0, 1, 1, 1, 0, 0)$, and the cell kinetics are due to normal physiological conditions. The order of the method is calculated from

$$\|u - u_\Delta\|_2 = C\Delta t^\alpha,$$

where C is the proportionality factor and α is the rate. Table 2 shows simulations for initial values that typically occur during shock, i.e. we have set $(v, c, m, h, j, f, d, X)_{t=0} = (800, 3.9 \cdot 10^{-27}, 1, 1, 1, 1, 0, 1)$. Observe that the convergence is satisfactory for these initial conditions as well.

Δt	1.order scheme			2.order scheme		
(ms)	error	rate	constant	error	rate	constant
2^{-3}	27.51	0.72	220	1.59	2.17	144
2^{-4}	15.60	0.82	249.5	3.86e-01	2.04	111
2^{-5}	8.34	0.90	267.3	9.60e-02	2.01	101
2^{-6}	4.32	0.95	276.7	2.40e-02	2.00	99.1
2^{-7}	2.20	0.97	281.7	5.99e-03	2.00	98.4
2^{-8}	1.11	0.99	284.4	1.50e-03	2.00	98.2
2^{-9}	0.56	1.03	278.6	3.74e-04	2.00	98.1

TABLE 2. Errors at $t = 10$ (ms) for the initial data $(v = 800, c = 3.9 \cdot 10^{-27}, m = 1, h = 1, j = 1, X = 1, d = 0, f = 1)$.

As a final convergence test, we run the simulations for an entire action potential, i.e. for $t \in [0, 400]$ ms, to see whether the order of convergence is preserved. Table 3 contains the convergence results for several Δt and we observe that the scheme shows its designed second order accuracy for small time steps as expected.

Finally we illustrate the accuracy of the solver by plotting the action potential from $t \in [0, 400]$ms, with $\Delta t = 2.0$ms. Figure 1, left part, shows plots of v using the

$\frac{\Delta t}{10}$ (ms)	l_2-error	l_2-order	error-constant
2^{-1}	2.42e-01	3.34	1.12e-3
2^{-2}	5.59e-02	2.12	8.05e-3
2^{-3}	1.07e-02	2.38	6.28e-3
2^{-4}	2.64e-03	2.02	6.82e-3
2^{-5}	5.98e-03	-1.18	1.51e-3
2^{-6}	2.75e-03	1.12	2.20e-2
2^{-7}	1.23e-04	4.48	11.2
2^{-8}	3.76e-05	1.71	9.69e-3
2^{-9}	7.83e-06	2.26	5.82e-2
2^{-10}	2.15e-06	1.87	1.22e-2
2^{-11}	5.96e-07	1.85	1.11e-2
2^{-12}	1.59e-07	1.91	1.55e-2
2^{-13}	4.10e-08	1.95	2.00e-2

TABLE 3. Errors at $t = 400$ (ms) for the initial data $(v = -40, c = 0.0002, m = 0, h = 1, j = 1, X = 0, d = 0, f = 1)$.

scheme studied in this paper compared to the fine solution (dotted line), as well as

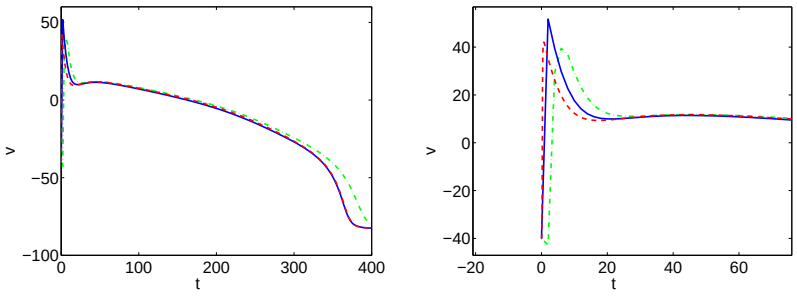

FIGURE 1. The transmembrane potential, fine solution $(--)$ and the second order scheme scheme $(-)$ using $\Delta t = 2.0$ms. A first order scheme is included for comparison.

that of an unconditionally stable first order scheme presented in [4]. In the right plot we have zoomed in on the up-stroke, and we observe how closely the solution computed with the second order method follows the fine solution.

6. Concluding remarks

As we have seen in this paper, it is possible to derive a second order accurate and unconditionally stable numerical method for an ODE model used in simulations of cardiac defibrillation. The traditional semi-implicit methods fail both concerning accuracy since they are only of order $O(\Delta t)$, and in terms of efficiency due to the small time steps needed. For instance, the well-established Crank-Nicolson scheme is impractical for the present application, due to the extremely strict time step condition. Here we have proposed a method that is fairly straightforward to implement. We remark that the two steps outlined in Section 3 can easily be carried over to larger ODE systems with a higher level of realism. State of the art

models would however, involve more ODEs with complicated nonlinear terms, so the algorithm implementation would generally require more effort.

Appendix A. Gate variable rate functions and parameters

Below we have listed the rate functions α_y, β_y, for $y = m, h, j, f, d, X$. Note that the opening and closing rates of h and j are smoothed out in order to obtain the desired level of accuracy, see discussion in Section 2. We have used a least-squares method in MATLAB to fit the new curve to data obtained from the original rate functions. The new functions are on the form originally standardized by Noble, see [9], i.e.

$$\alpha_{h,j}, \beta_{h,j}(v) = \frac{(c_1 \exp(c_2(v - c_6)) + c_3(v - c_6))}{(c_4 \exp(c_5(v - c_6)) + 1)}. \tag{40}$$

The other rate functions appear as follows:

$$\alpha_m = \frac{0.32(v + 47.13)}{1 - \exp[-0.1(v + 47.13)]} \qquad \beta_m = 0.08 \exp(\frac{-v}{11.0})$$

$$\alpha_h = 0.085 \exp(-0.15(V + 77)) \qquad \beta_h = \frac{7.7}{\exp(-0.1(V + 11.5)) + 1}$$

$$\alpha_j = \frac{0.053 \exp(-0.15(V + 78))}{\exp(-0.047(V + 78)) + 1} \qquad \beta_j = \frac{0.3}{\{\exp(-0.1(V + 32)) + 1\}}$$

$$\alpha_d = \frac{0.095 \exp[-0.01(v - 5)]}{1 + \exp[-0.072(v - 5)]} \qquad \beta_d = \frac{0.07 \exp[-0.017(v + 44)]}{1 + \exp[-0.05(v + 44)]}$$

$$\alpha_f = \frac{0.012 \exp[-0.008(v + 28)]}{1 + \exp[0.15(v + 28)]} \qquad \beta_f = \frac{0.0065 \exp[-0.02(v + 30)]}{1 + \exp[-0.2(v + 30)]}$$

$$\alpha_X = \frac{0.0005 \exp[-0.083(v + 50)]}{1 + \exp[0.057(v + 50)]} \qquad \beta_X = \frac{0.0013 \exp[-0.06(v + 20)]}{1 + \exp[-0.04(v + 20)]}$$

$$K1_\infty = \frac{\alpha_{K1}}{\alpha_{K1} + \beta_{K1}} \qquad K_p = \frac{1}{1 + \exp[7.488 - v/5.98]}$$

$$\alpha_{K1} = \frac{1.02}{1 + \exp[0.2385(v - E_{K1}) - 59.215]}$$

$$\beta_{K1} = \frac{0.49124 \exp[0.08032(v - E_{K1} + 5.476)] + \exp[0.06175(v - E_{K1} - 594.31)]}{1 + \exp[-0.5143(v - E_{K1} + 4.753)]}$$

A note on the inactivation gate of I_K

The delayed rectifier current, I_K of the LR1 model is, as described above, governed by

$$I_K = g_K X X_i (v - E_K).$$

As proposed by Shibasaki [12], X and X_i are respectively the activation and the inactivation gates. The latter is clamped at $X_i = 1$, i.e.

$$X_i = \frac{2.837(\exp(0.04(v + 77)) - 1.0)}{(v + 77)\exp(0.04(v + 35))}, \quad v \geq -100,$$
$$X_i = 1.0, \quad \text{otherwise.}$$

Observe that this gate is clamped at $v \leq -100$mV. For simulations of electrical pulse propagation under normal conditions, this singularity will be outside the range of v, and thus not affect the order of accuracy. However, in simulations of defibrillation, the tissue will be hyperpolarized down to such an extent that the break point will

be crossed and the second order accuracy can not be obtained. Therefore we have chosen to approximate the inactivation gate with a smooth version. Since X_i is set to its steady state, we propose

$$X_i = \frac{\alpha_{X_i}}{\alpha_{X_i} + \beta_{X_i}} \tag{41}$$

where the opening and the closing rates are on the form (40). The parameters in Table 4 are found by using the same method as was done for the other rate functions. Figure 2 shows the original X_i function together with the smooth version, left part,

	c_1	c_2	c_3	c_4	c_5	c_6
α_{X_i}	$5.458 \cdot 10^5$	0.04554	-0.046	$1.05 \cdot 10^7$	0.0495	166.5
β_{X_i}	0.55	0.028	0.001017	1.175	0.0283	-55

TABLE 4. Coefficients for smooth version of the X_i-gate on the form given in (41).

and the effect on the AP, right part. Observe the minimal difference in the action

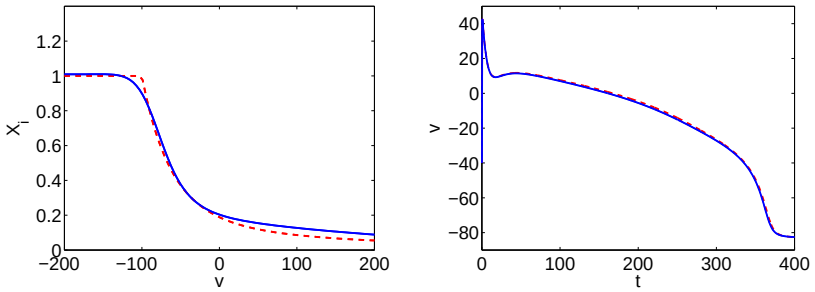

FIGURE 2. Left plot: The original X_i gate, $(--)$, and the smooth version$(-)$. Right plot: The effect of a smooth X_i on the transmembrane potential; original $(--)$, and smoothed version $(-)$.

potential for the new rate function. Finally, in Table 5 we list the conductivity constants and the equilibrium potentials of the membrane currents, see [8].

References

[1] G.W Beeler and H. Reuter, Reconstruction of the action potential of ventricular myocardial fibres, *J of Physiol.*, 268(1977) 177-210.

[2] K. A. DeBruin and W. Krassowska, Modeling Electroporation in a single cell. II. Effects of ionic concentrations., *Biophys J*, 77(1999) 1225-1233.

[3] P.C Franzone, L. Guerri and S. Rovida, Wavefront propagation in an activation model of the anisotropic cardiac tissue: asymptotic analysis and numerical simulations, *J of Math Biol*, 28(1990) 121-176.

[4] M. Hanslien, J. Sundnes and A. Tveito, An unconditionally stable numerical numerical method for the Luo-Rudy 1 model used in simulations of defibrillation, *Mathematical Biosciences*, 208(2) 375-392, 2007.

[5] J. Keener and J. Sneyd. Mathematical physiology, volume 8. Springer, 1980.

[6] W. Krassowska, Effects of electroporation on transmembrane potential induced by defibrillation shocks, *PACE*, 18(1995) 1644-1660.

[7] W. Krassowska and K. A. DeBruin, Modeling electroporation in a single cell. I. Effects of field strength and rest potential, *Biophys J*, 77(1999) 1213-1224.

E_{Na}	54.4 mV
E_K	-77.0 mV
E_{K1}	-87.185 mV
E_{K_p}	-87.185 mV
E_b	-59.87 mV
g_s	0.09 mS/cm^2
g_{Na}	23.0 mS/cm^2
g_K	0.282 mS/cm^2
g_{K1}	0.6047 mS/cm^2
g_{Kp}	0.0183 mS/cm^2
g_b	0.03921 mS/cm^2

TABLE 5. Constants appearing in the LR1 model.

[8] C. H. Luo and Y. Rudy, A model of the ventricular cardiac action potential: depolarization, repolarization and their interaction, *Circ. Res.*, 68(1991) 1501-1526.
[9] D. Noble, A modification of the Hodgkin-Huxley equations applicable to Purkinje fiber action and pacemaker potential, *J of Physiol*, 160(1962) 317-352.
[10] Z. Qu and A. Garfinkel, An advanced algorithm for solving partial differential equation in cardiac conduction., *IEEE Trans Biomed Eng*, 46(9) 1166-1168,1999.
[11] S. Rush and H. Larsen, A practical algorithm for solving dynamic membrane equations, *IEEE Trans Biomed Eng*,25(1978) 389-392.
[12] T. Shibasaki, Conductance and kinetics of delayed rectifier potassium channels in nodal cells of the rabbit heart, *J of Physiol*,387(1987) 227-250.
[13] J. Sundnes, G. T. Lines and A. Tveito, An operator splitting method for solving the bidomain equations coupled to a volume conductor model for the torso, *Mathematical Biosciences*, 194(2) 233-248, 2005.
[14] L. Tung, A Bi-domain model for describing ischemic myocardial D-C potentials, *PhD thesis, MIT, Cambridge, MA*, 1978.

Department of Scientific Computing, Simula Research Laboratory,P.O.Box 134, N–1325 Lysaker, Norway
E-mail: monicaha@simula.no
URL: www.simula.no/people